Translational Oncology
www.transonc.com

Volume 11 Number 4 August 2018 pp. 900–910 900

Hydrogen Sulfide Demonstrates Promising Antitumor Efficacy in Gastric Carcinoma by Targeting MGAT5[1,2]

Rui Wang[*,3], Qilin Fan[†,3], Junjie Zhang[†], Xunan Zhang[‡], Yuqi Kang[§] and Zhirong Wang[†]

[*]Shanghai Key Laboratory of Bioactive Small Molecules and Research Center on Aging and Medicine, Department of Physiology and Pathophysiology, Fudan University Shanghai Medical College, Shanghai, China; [†]Department of Gastroenterology, Tongji Hospital Affiliated to Tongji University, Shanghai, China; [‡]Department of Medical Imaging, Tongji Hospital Affiliated to Tongji University, Shanghai, China; [§]Department of Medical Oncology, Oncology Hospital of Guizhou Province, Guizhou, China

Abstract

Mannosyl (alpha-1,6-)-Glycoprotein beta-1,6-N-acetyl-glucosaminyltransferase (MGAT5) is exclusively expressed in gastric carcinoma, and plays an essential role in cancer progression, but no targeted drug is available so far. The potential anti-cancer effect of Hydrogen Sulfide (H_2S), has not been widely recognized. It intrigued broad interest to explore the clinical benefits of cancer therapy, with the current understanding of molecular mechanisms of H_2S which remains very limited. In this study, we identify that H_2S is an effective inhibitor of MGAT5, leading to reduce the expression of exclusively abnormal glycoprotein processes in gastric carcinoma. H_2S specifically dissociation of karyopherin subunit alpha-2 (KPNA2) with Jun proto-oncogene (c-Jun) interaction, and blocking c-Jun nuclear translocation, and downregulation of MGAT5 expression at the level of gene and protein. Consequently, H_2S impairs growth and metastasis in gastric carcinoma by targeting inhibits MGAT5 activity. In an animal tumor model study, H_2S is well tolerated, inhibits gastric carcinoma growth and metastasis. Our preclinical work therefore supports that H_2S acts as a novel inhibitor of MGAT5 that block tumorigenesis in gastric carcinoma. *SIGNIFICANCE:* This study shows that H_2S can effective targeting inhibits MGAT5 activity, and demonstrates promising antitumor efficacy. These findings gain mechanistic insights into the anti-cancer capacity of H_2S and may provide useful information for the clinical explorations of H_2S in cancer treatment.

Translational Oncology (2018) 11, 900–910

Introduction

Gastric carcinoma (GC) is by far the leading fatal reason for death in developing country [1,2]. Although considerable effort has been directed toward the improvement of chemotherapeutic intervention, the 5-year survival rate of stomach neoplasm patients remains poor partly due to the development of Chemo-resistance, raising an urgent need to seek more effective treatment strategies [2].

MGAT5 is required in the biosynthesis of β1,6GlcNAc-branched N-linked glycans attached to cell surface and secreted glycoproteins. Amounts of MGAT5 glycan products are commonly increased in malignancies, and correlate with disease progression [3–7]. MGAT5 critically remodels tumor microenvironment to facilitate tumor cell growth and metastasis [8,9]. MGAT5 caused ECM collapse also led to release of glycosyl transferase binding cytokines like VEGF and MMPs, which promote tumor growth and metastasis [10]. Such an irreplaceable role in cancer growth and metastasis makes MGAT5 an appealing target for cancer therapy [11,12]. However, there is no MGAT5 inhibitor available in clinical to date.

Address all correspondence to: Zhirong Wang, MD, Department of Gastroenterology, Tongji Hospital Affiliated to Tongji University, Shanghai 200065, P.R. China.
E-mail: wangzr_tongji@163.com

[1] Grant Support: This work was supported by the Strategic Priority Research Program of the Science and Technology Commission of Shanghai (1312JC1408402 for Zhirong Wang).
[2] Disclosure of Potential Conflicts of Interest: No potential conflicts of interest were disclosed.
[3] These authors contributed equally to this work.
Received 1 March 2018; Revised 16 April 2018; Accepted 16 April 2018

1936-5233
https://doi.org/10.1016/j.tranon.2018.04.008

H_2S has been recognized along with nitric oxide (NO) and carbon monoxide (CO) [13,14]. A number of studies have shown that H_2S is involved in many physiological and pathophysiological functions [15–17]. However, the anti-tumor effect of H_2S has not been widely recognized and the current understanding of molecular mechanisms of H_2S remains very limited [18–20]. Hence, we identify H_2S associated proteins, and discovered MGAT5 as one of the potential targets of H_2S in gastric carcinoma by previous proteomic study.

This study aims to provide the proof-of-concept for evaluating MGAT5 inhibitors as antitumor agents, and to explore the role of H_2S inhibits MGAT5, and to demonstrate biological significance to complement pharmacological effects of H_2S.

Materials and Methods

Cell Culture

Human gastric cancer cells MKN45 and human normal gastric epithelial cells GES-1 were purchased from American Type Culture Collection (ATCC). Human gastric cancer cells BGC823 and human gastric cancer cells BGC803 were obtained from the Institute of Tongji Hospital Affiliated to Tongji University. All the cell lines used in this study were obtained during 2000 to 2012 and cultured according to the suppliers' instructions. Cells were checked and confirmed to be mycoplasma-free, and the cells were passaged no more than 25–30 times after thawing. Cell lines were characterized by Genesky Biopharma Technology using short tandem repeat (STR) markers.

cAMP Activity Assay

Briefly, 1.0 mL compound and 4.0 ml of cAMP solution or 5.0 ml cAMP dilution buffer were added to 96 well plate. After 10 minutes preincubation at 37°C, an enzyme reaction was initiated by adding 5.0 ml of Bio-HS-Eu (K) (Cisbio International) and the 96 well plate was incubated for 150 minutes at 37°C. To stop the enzyme reaction and detect the remaining substrate, either 10 ml of a 1.0 mg/ml XL665-labeled streptavidin (Cisbio International) solution or dilution buffer was added to the plate. After a 30 mins incubation at RT, the Homogeneous Time Resolved Fluorescence (HTRF) signal was measured using an Envision plate reader (Perkin Elmer).

MGAT5 Activity Assay

Briefly, MGAT5 activity was assayed in the separate tube in the absence of $MnCl_2$. After incubation at 37°C for 5 hours, the reactions were stopped by heating at 100°C for 3 mins and the samples were centrifuged at 5000 rpm in an Eppendorf tube for 15 min. An aliquot (20 μl) of each sample was applied to ODS C_{18} column to separate the products of MGAT5 from the acceptor substrate by High Performance Liquid Chromatography (HPLC) method. All the samples were assayed in duplicate. The enzyme activities were calculated according to the peak areas of the products and expressed as GlcNAc (pmol) transferred/h/mg protein.

Wound Healing Assay

Confluent human gastric cancer cells were starved overnight and were scratched using a pipette tip for the wound healing assay. Markings were drawn on the culture dishes as reference points so as to make sure that the same visual field was photographed at 0 hour and 24 hours. Typically, 8–12 visual fields were chosen randomly in one culture dish. Cells were photographed using an EVOS fl Microscope (Advanced Microscopy Group, Mill Creek, Washington) after incubation, according to the suppliers' instructions. The outline of the wound area (the area with no cells) was then drawn using Image J software to get the exact pixel coverage of each wound area.

Cell Invasion Assay

Transwell chambers (8 μm pore size; Corning Life Sciences, Lowell, MA) were coated with 100 μl of diluted matrigel. 0.6 ml medium containing 20% FBS was added to the lower chambers, and cells suspended in serum-free medium at a density of 1.5×10^5 cells/ml (doubled for invasion) were seeded (0.1 ml) in the upper chambers. Various concentrations of aspirin were added to both of the upper and lower chambers. After cultured for an appropriate time (24 hours), cells were then fixed by cold 95% ethanol, stained by 0.1% crystal violet, and cells that had not migrated were removed from the upper chambers. The remaining cells were photographed. The dye was dissolved in 80 μl of 10% acetic acid, and the absorbance of the resulting solution was measured at 600 nm using a multiwell spectrophotometer.

Western Blotting

Cell lysates were determined with Bicinchoninic acid (BCA) method, and an equal amount of proteins was separated by SDS–PAGE and then transferred to nitrocellulose membranes. The membranes were blocked with 5% (w/v) non-fat dry milk, followed with overnight incubation at 4°C with the following antibodies which were provided in the Supplemental Table 1. Immunoreactive proteins were detected using ECL Plus (Thermo Fisher Scientific, Waltham, MA), after secondary antibody incubation.

Apoptosis Assay

Cells were seeded into 35 mm dishes (1×10^5 cells/dish) and treated with NaHS, or PBS. The cells were fixed and analyzed by flow cytometry (FACS) (BD FACS Array Bioanalyzer). Apoptotic cells were stained using the Apo-Alert Annexin V kit (BD Biosciences) before analysis.

Immunofluorescence Staining

Cells were fixed with 4% paraformaldehyde at 4°C for 10 min. After washing and pre-blocking, the cells were incubated at 4°C overnight with antibodies against Monoclonal anti-human c-Jun and Monoclonal anti-human MGAT5, respectively, followed by incubation with the FITC-conjugated secondary antibody (1:50; CST) for 1 hour. DAPI was used for nuclear staining (10 μg/ml in PBS, Invitrogen, Life Technologies). Images were then analyzed by laser confocal microscopy (Leica Sp5 Laser Scanning Confocal Microscope; GE).

RNA Extraction, Quantitative Real-Time PCR

Total RNA samples from cultured cells were extracted using Trizol reagent (Invitrogen) according to the manufacturer's instructions. The sequences of the primers are listed in Supplemental Table 2. Quantitative real-time PCR (qRT-PCR) was performed using an ABI PRISM 7500 Sequence Detection System (Applied Biosystems). The housekeeping gene glyceraldehyde-3 phosphate dehydrogenase (GAPDH) was used as an internal quantitative control.

Chromatin Immunoprecipitation (ChIP) Assays

The ChIP assay was performed according to the protocol described previously. In brief, after treatment, BGC823, MGC803, and MKN45 cells were treated with 1% formaldehyde for 10 min to

crosslink chromatin and protein. The chromatin-protein samples were immunoprecipitated with c-Jun antibody. The immunoprecipitates were then incubated with protein A/G agarose beads. After several washes, the protein–DNA complex was reversed. DNA was purified using phenol-chloroform. The DNA was analyzed by qPCR using primers that were specific for regions spanning the c-Jun binding sites in the promoters of *MGAT5*.

Electrophoretic Mobility Shift (EMSA) Assay

Nuclear extracts were isolated from cells with or without NaHS treatment. Nuclear proteins were mixed with biotin-labeled probes containing the AP-1 consensus sequence and incubated at room temperature for 20 min. The sequences of the biotin-labeled probes are listed in Supplemental Table 3. The protein-DNA mixtures were then separated from the free probe on 6% polyacrylamide gel in a 4°C-cold room for 2 hours in Tris-glycine-EDTA running buffer. The gel was dried, exposed to films, and analyzed by a Phosphor Imager (Amersham Biosciences).

AP-1 Luciferase Reporter Assay

Luciferase reporter assay was performed using a Dual-Luciferase Reporter Assay System (Promega). Luciferase reporters were transfected into cells cultured in 35 mm dishes with or without NaHS treatment as described.

2-Deoxyglucose Uptake

Uptake of 2-deoxyglucose by the human GC cell lines BGC823 was measured as previously described after the treatment with NaHS at doses (100 μM) for 24 h. The cells were rinsed with a KRP buffer (128 mM NaCl, 4.7 mM KCl, 1.25 mM $CaCl_2$, 1.25 mM $MgSO_4$, 5 mM NaH_2PO_4, 5 mM Na_2HPO_4, and 10 mM HEPES, pH 7.4), containing 0.1% (w/v) BSA and 5 mM glucose every 40 min for a total of 120 min at 37°C. The cells were then treated with 100 nM insulin in a KRP buffer without glucose for 15 min or left untreated. 2-deoxy-D [^{3}H]-glucose (1 $\mu Ci \cdot ml^{-1}$) was added, and the cells were incubated for 15 min. The cells were rinsed three times in ice-cold phosphate-buffered saline (PBS) containing 10 mM glucose, and they were then lysed with 0.4 N NaOH. ^{3}H radioactivity was measured in a liquid scintillation counter (Beckman LS6500). Each sample was measured in triplicate. Nonspecific uptake was determined in the presence of cytochalasin B (10 μM) and was subtracted from each value. A transient treatment (15 min) with 100 nM insulin in the KRP buffer before the cells were treated with radioactive glucose was applied in both the cells cultured with low glucose (5.5 mM, without insulin) and the cells cultured with high glucose (25 mM) with insulin (100 nM). In these experiments, the concentration of insulin applied in the following glucose-uptake assay (including the transient insulin treatment before application of 2-deoxy-d [^{3}H]-glucose and the insulin contained after application of 2-deoxy-D[^{3}H]-glucose) was identical to that used in the cell culture period.

XF Bioenergetics Assay

Mitochondrial oxygen consumption rate (OCR), extracellular acidification (ECAR) and Fatty acid oxygen (FAO) were conducted using a Seahorse XF24 Analyzer. The cells were seeded in Seahorse 24-well microplates and cultured at 37°C with 5% CO_2. The following day, the media was replaced with 700 μl assay medium composed of DMEM without FBS and sodium bicarbonate and incubated at 37°C without CO_2 for 1 hour. The basal OCR and ECAR were measured. To measure cells mitochondrial capacity, drugs were injected to the final concentration as 2 μg/ml of oligomycin, 2.5 μM of carbonylcyanide-ptrifluorometthoxyphenyl-hydrazone (FCCP) and 2 μM of antimycin A. To measure cells glycolytic capacity, the drug was injected to a final concentration as 11 mM glucose, 20 mM 2-DG.

Co-Immunoprecipitation

Cells were collected with NP40 cell lysis buffer. An equal amount of proteins was incubated with antibodies overnight at 4°C. Immunoprecipitates were incubated with protein A/G agarose beads and non-specific proteins were washed away by wash buffer.

Immunohistochemistry

Immunohistochemistry (IHC) was performed on tumor sections from human GC cells BGC823 orthotopic Xenotransplantation in nude mice, using antibodies listed in the supplementary materials and methods.

Xenograft Tumor Model

This animal study was conducted in accordance with the rules and regulations of the Institutional Animal Care and Use Committee (IACUC) at the Department of Laboratory Animal Science, Fudan University (Shanghai, P.R. China). Male Balb/c nude mice, 4 to 5 weeks old, were purchased from Shanghai SLAC Laboratory Animal Limited Company. Tumor cells at a density of 5×10^6 in 0.2 ml PBS were injected subcutaneously into the stomach of nude mice. The mice were randomly assigned to two groups, control (0.9% saline), NaHS treatment 100 μM/Kg. Body weight of mice was measured individually triple per day. After treatment for two weeks (15 days), mice were sacrificed after the final therapy, and lungs were fixed in 4% paraformaldehyde.

Statistical Analysis

Data are presented as the mean–standard deviation. If variances were homogeneous, differences were assessed by one-way ANOVA. Spearman's rank test and Fisher's exact test were used to analyze clinicopathological correlation. All statistical analyses were carried out using SPSS version 16.0. A two-tailed p-value of <0.05 was considered as statistically significant. Student's t-tests were performed as indicated in the figures. Results were considered significant when $P < .05$.

Results

H_2S Downregulates the Expression of MGAT5 and Inhibits its Activity

MGAT5 is an enzyme that catalyzes the formation of a β1,6-N-acetylglucosamine side chain to a core mannosyl residue in N-linked glycoproteins. Besides its direct function of producing aberrant glycoproteins, it promotes cancer progression by its involvement in the stimulation of oncoproteins in cancer cells [6,21–24]. It has recently emerged as a promising target for cancer therapy [12].

In a previous effort to identify the potential targets of H_2S in gastric carcinoma (GC), we conducted a proteomic study to identify a novel MGAT5 inhibitor. Sodium Hydrosulfide (NaHS) is a donor, which rapidly releases H_2S. We first found the *MGAT5* gene level and MGAT5 protein level was apparent diminution observed in GC cells treated with NaHS for 24 hours (Figure 1A, B). Immunofluorescence confocal also show, the expression of MGAT5 was apparent

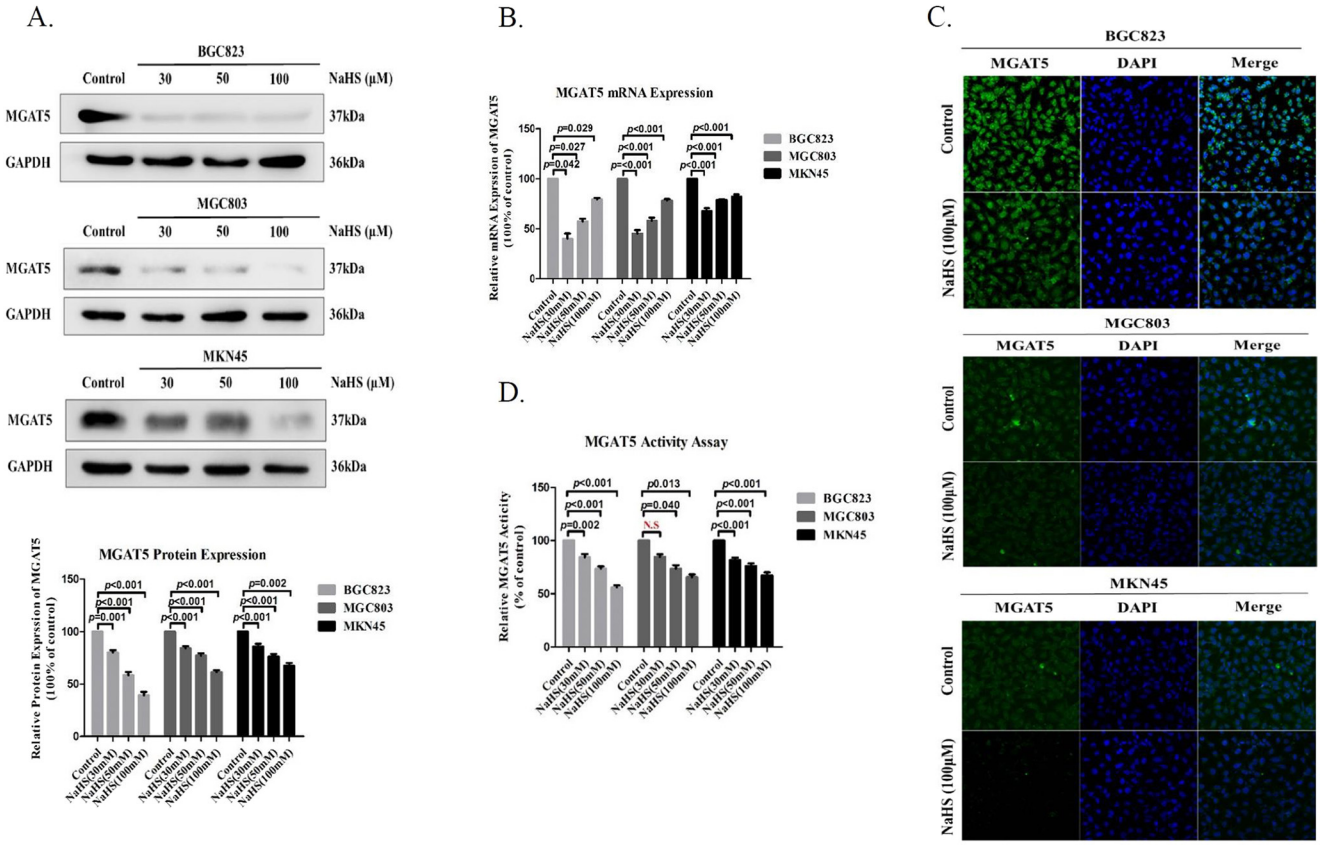

Figure 1. H_2S downregulates the expression of MGAT5 and inhibits its activity.(A). After treatment with various concentrations of NaHS for 24 h, cell extracts were prepared and applied to immunoblotting with MGAT5. GAPDH was used as a loading control. (B). quantitative real-time PCR analysis the expression of *MGAT5* mRNA in GC cells after 24 hours with treatment NaHS at various concentrations. (C). Immunofluorescence staining of MGAT5 in GC cells treated with NaHS at 100 μM after 24 hours. (D). The effect of H_2S on MGAT5 activity inhibition in different cells. Various concentrations of NaHS were added to GC cells. The activity of MGAT5 was determined by the HPLC methods using pyridiylaminated $GlcNAc_2Man_3GlcNAc_2$ as acceptor substrate in the absence of Mn^{2+}. Each bar represents the means ± S.D. of three independent experiments.

diminution observed in the GC cells treated with NaHS for 24 hours (Figure 1C). To further confirm the MGAT5 activity inhibitory effect with NaHS treatment, we detected the activity of MGAT5 by HPLC assay with the same amount of protein in GC cells at the same time with NaHS treatment on different concentrations. We found the H_2S significantly inhibited the activity of MGAT5 in GC cells (Figure 1D). The aforementioned results suggested the potential function of H_2S on inhibiting cellular MGAT5 activity in GC cells.

H_2S Inhibits MGAT5 Activity Though Specifically Dissociation of KPNA2 With c-Jun Interaction

To further establish whether H_2S exclusively inactivated c-Jun, ETS Proto-Oncogene 1 (ETS-1), Transcription Factors of the Nuclear Factor KB (NF-KB), bHLH Transcription Factor (c-Myc), Hypoxia Inducible Factor 1 alpha subunit (HIF-1 alpha), and Mammalian Target of Rapamycin (mTOR) signaling pathway were evaluated [24–30]. In GC cells, the status of c-Jun, ETS-1, NF-KB, c-Myc, HIF-1a remained unchanged after addition of NaHS for 24 hours (Figure 2A, Supplementary Figure S2A). At the same time, we found the H_2S promoted an increased cellular level of the cAMP in GC cells by HTRF assay (Figure 2B). Results suggested the potential function of H_2S on inhibiting cellular mTOR signaling pathway in GC cells [30]. Indeed, treatment of NaHS with GC cells led to a dose-dependent inhibition of cellular mTOR signaling pathway by western blot assay (Figure 2C, Supplementary Figure S2B). Afterwards, we found that the cAMP-dependent inhibition of mTOR signaling pathway could be mediated by upregulated AMPK activation in GC cells (Figure 2C). Moreover, we found the protein level of KPNA2 was apparent a concentration-dependent diminution observed in the cell extracts from GC cells treated with NaHS for 24 hours (Figure 2A). After that, we detected the relationship between KPNA2 and c-Jun with NaHS treatment. Co-IP detection show, KPNA2 and c-Jun is interaction each other (Figure 2D). Afterwards, we found that the c-Jun has no apparent change in the whole cell extracts from GC cells treated with NaHS for 24 hours (Figure 2A), and that there was a concentration-dependent augmentation of c-Jun in the GC cells cytoplasm, with a progressive diminution in the GC cells nuclei (Figure 2E). Immunofluorescence confocal show, c-Jun is obviously blocked in the cytoplasm from nuclear with treatment NaHS for 24 hours in GC cells, compared with control (Figure 2F). We further examined the relationship between H_2S and AP-1 activity by transfection of DNA constructs containing an AP-1 promoter region into GC cells. As shown luciferase reporter assay, H_2S significantly augmented AP-1 promoter luciferase activity in GC cells (Figure 2G). The inhibitory effect of H_2S on AP-1 binding activation was validated by EMSA, in which

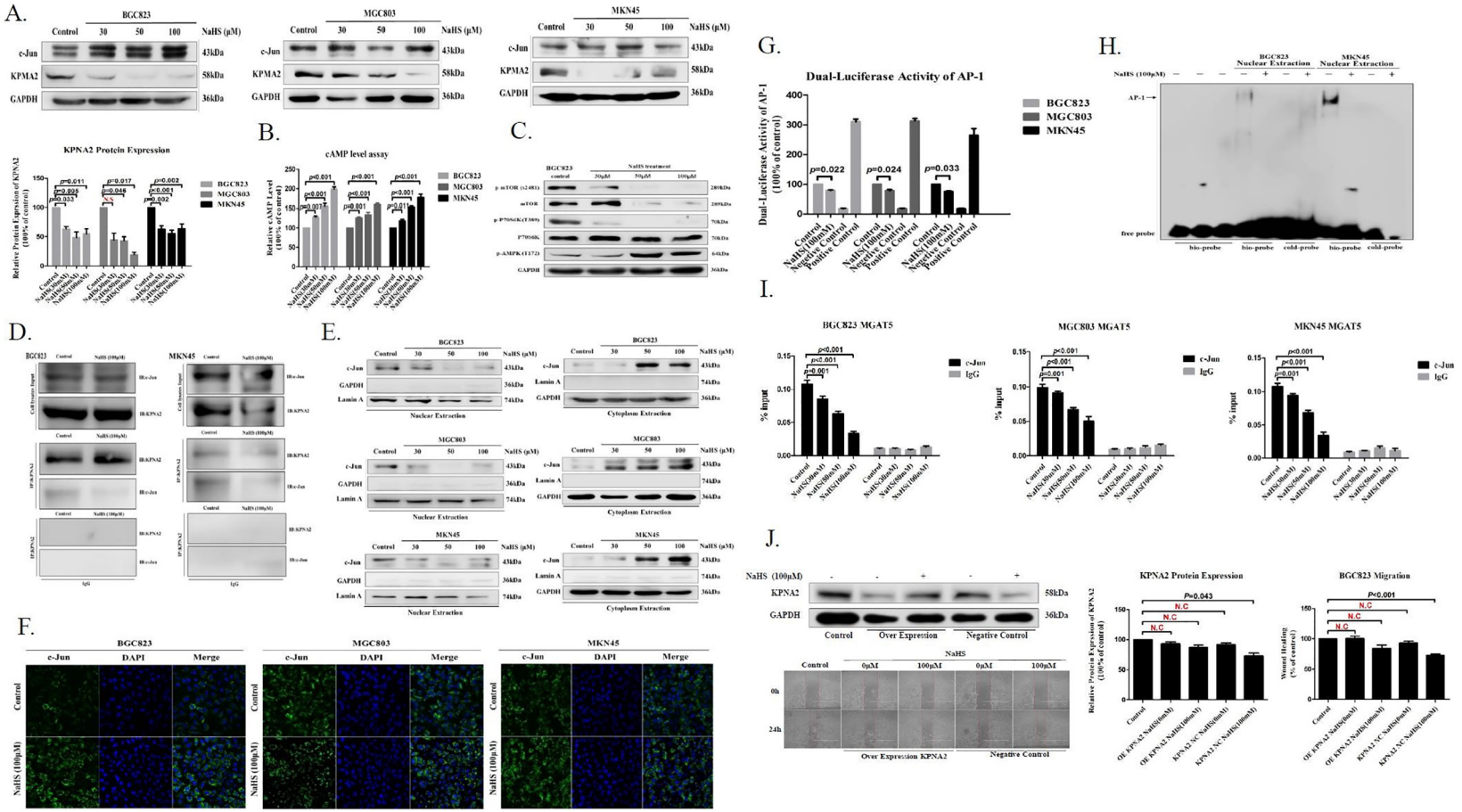

Figure 2. H_2S inhibits MGAT5 activity though specifically dissociation of KPNA2 with c-Jun interaction.(A). After treatment with various concentrations of NaHS for 24 h, cell extracts were prepared and applied to immunoblotting with c-jun and KPNA2. GAPDH was used as a loading control. (B). The cAMP activity was assayed by HTRF. Various concentrations of NaHS were added to GC cells. (C). Western blotting of protein on the mTOR signaling pathway in BGC823 cells after 24 hours with NaHS treatment indicated various concentrations. GAPDH was used as a loading control. (D). Co-Immunoprecipitation detection the relationship between KPNA2 and c-Jun with NaHS treatment after 24 hours in BGC823 and MKN45. (E). Western blotting assayed c-Jun from nuclear and cytoplasmic extracts of GC cells treated with various concentrations for 24 hours. Lamin A and GAPDH was used as a loading control. (F). Immunofluorescence staining of c-Jun in GC cells treated with NaHS at 100 μM after 24 hours. (G). Luciferase reporter assay measuring AP-1 activity in GC cells transiently co-transfected with pAP-1-Luc with NaHS treatment for 24 hours at 100 μM. (H). EMSA assay of DNA binding to AP-1 in the nuclei extracts from BGC823 and MKN45 cells after NaHS treatment for 24 hours at 100 μM. Results are repetitive from at least two independent experiments. (I). GC cells were incubated with NaHS and analyzed by a quantitative ChIP assay with anti-c-Jun antibody. (J). The inhibitory effect of H_2S on migration of serum free stimulated stably KPNA2 over-expression in BGC823. Each bar represents the means $\pm$ S.D. of three independent experiments.

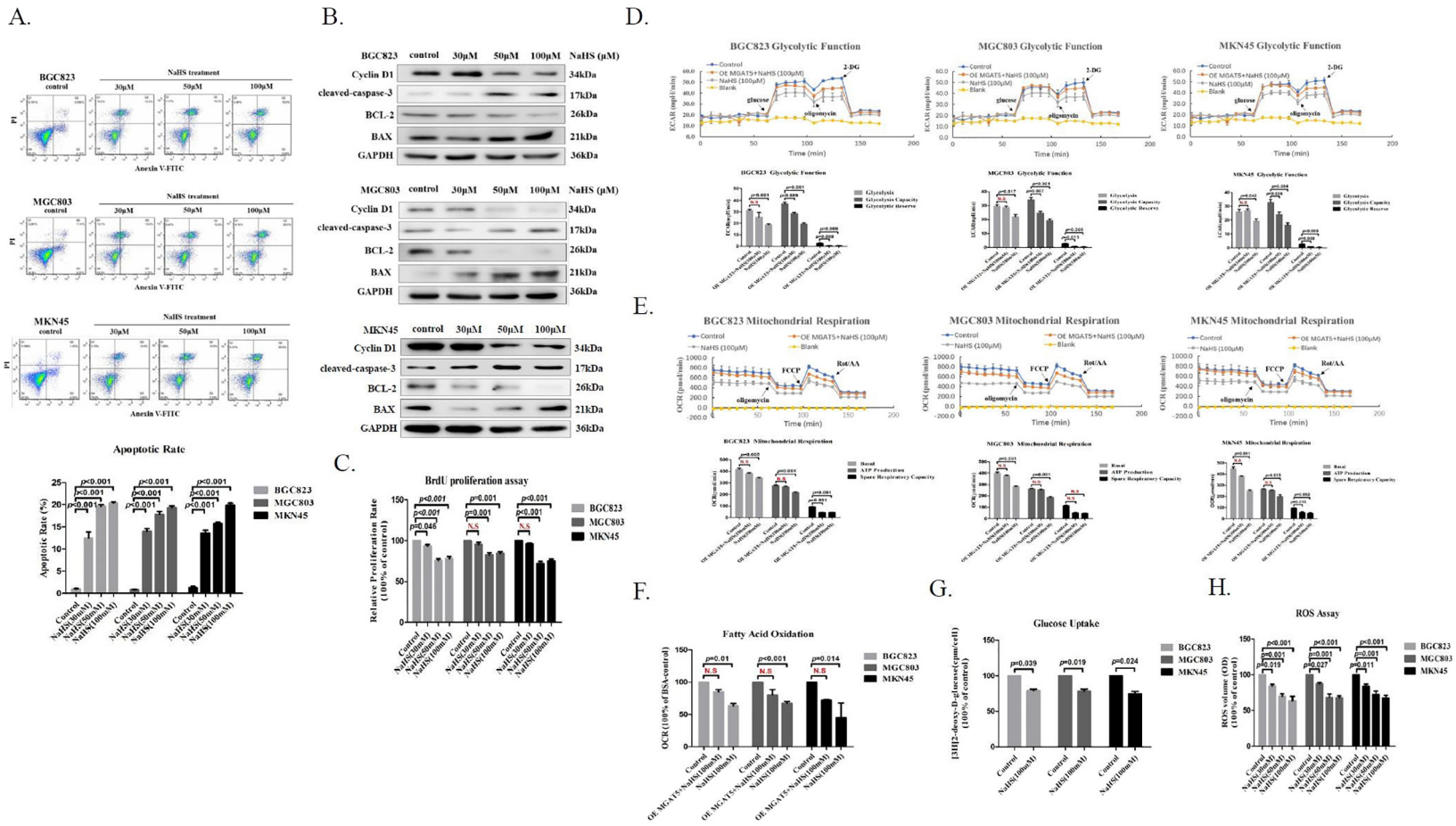

Figure 3. H_2S suppresses MGAT5-promoted GC cells growth.(A). FACS analysis of apoptosis in GC cells after 24 hours with treatment NaHS at various concentrations. (B). After treatment with various concentrations of NaHS for 24 h, cell extracts were prepared and applied to immunoblotting with apoptosis relevant protein. GAPDH was used as a loading control. (C). BrdU proliferation assay measuring GC cells proliferation capacity with NaHS treatment on various concentrations. Seahorse XF24 Extracellular Flux Analyzer examined the inhibitory effect of H_2S on cellular metabolism capacity of serum free stimulated stably MGAT5 over-expression in GC cells with NaHS treatment for 200 minutes at 100 μM. (D). Glycolytic Function. (E). Mitochondrial Respiration. (F). Fatty Acid Oxidation. (G). The effect of NaHS solution on 2-deoxtglucose uptake in GC cells. (H). Chemiluminescence analysis assayed the level of ROS in GC cells after 24 hours with treatment NaHS at various concentrations. Each bar represents the means ± S.D. of three independent experiments.

the DNA binding capacity of AP-1 in the nuclei extracted from BGC823 and MKN45 cells was attenuated by NaHS treatment for 24 hours (Figure 2I). ChIP assay further revealed that H_2S disturbed interaction between c-Jun and its target genes *MGAT5* in GC cells (Figure 2I). The aforementioned results showed that H_2S perturbed nuclear translocation and DNA-binding activity of c-Jun might have caused by specifically dissociation of KPNA2 with c-Jun interaction. To test whether the H_2S abrogated nuclear translocation and DNA-binding activity of c-Jun *via* specifically dissociation of KPNA2 with c-Jun interaction, we examined the impact on migration of BGC823 cells stably expressing KPNA2. We found that KPNA2 overexpression decreased the inhibitory effect on BGC823 cells migration with H_2S treatment (Figure 2J). In conclusion, our results demonstrated that H_2S inhibited MGAT5 activation *via* specifically dissociation of KPNA2 with c-Jun interaction, and repressed the expression of c-Jun downstream targets gene *MGAT5* in GC cells.

H_2S Suppresses MGAT5-Promoted GC Cells Growth

First, Flow cytometry analysis demonstrated that NaHS treatment caused a significant increase in the percentage of late apoptotic in GC cells (Figure 3A). More than that, Western blotting tested that NaHS treatment of GC cells enhanced the expression of BAX, activated caspase-3, two critical proteins indicating cellular apoptosis and suppressed the expression of Bcl-2, the key protein indicating cellular proliferation (Figure 3B). Bromodeoxyuridine (BrdU) proliferation assay also showed that H_2S significantly inhibited MGAT5-promoted GC cells proliferation on different concentrations (Figure 3C). Aerobic glycolysis is a hallmark of cancer, cancer cell get energy quickly through glycolysis, and the intermediate products produced by glycolysis are used for the synthesis of biological macromolecules required for proliferation [31–34]. To determine the reason behind this increase in the percentage of the late apoptotic, we next examined cellular metabolism capacity with treated NaHS. We measured ECAR, OCR, and FAO in GC cells treated with NaHS. We found that H_2S significantly suppressed glycolysis function, ATP production and fatty acid oxidation in GC cells treated with NaHS (Figure 3D, E, F, Supplementary Figure S3A). The aberrant glycoproteins lead to metabolic reprogramming in cancer cell [35]. This shift is mediated by an excessive increase in MGAT5 activity, thereby driving the tumor phenotype and promoting tumor growth [11,36,37]. We found that H_2S significantly reduced glucose uptake by 2-deoxyglucose uptake assay in GC cells (Figure 3G). We also detected

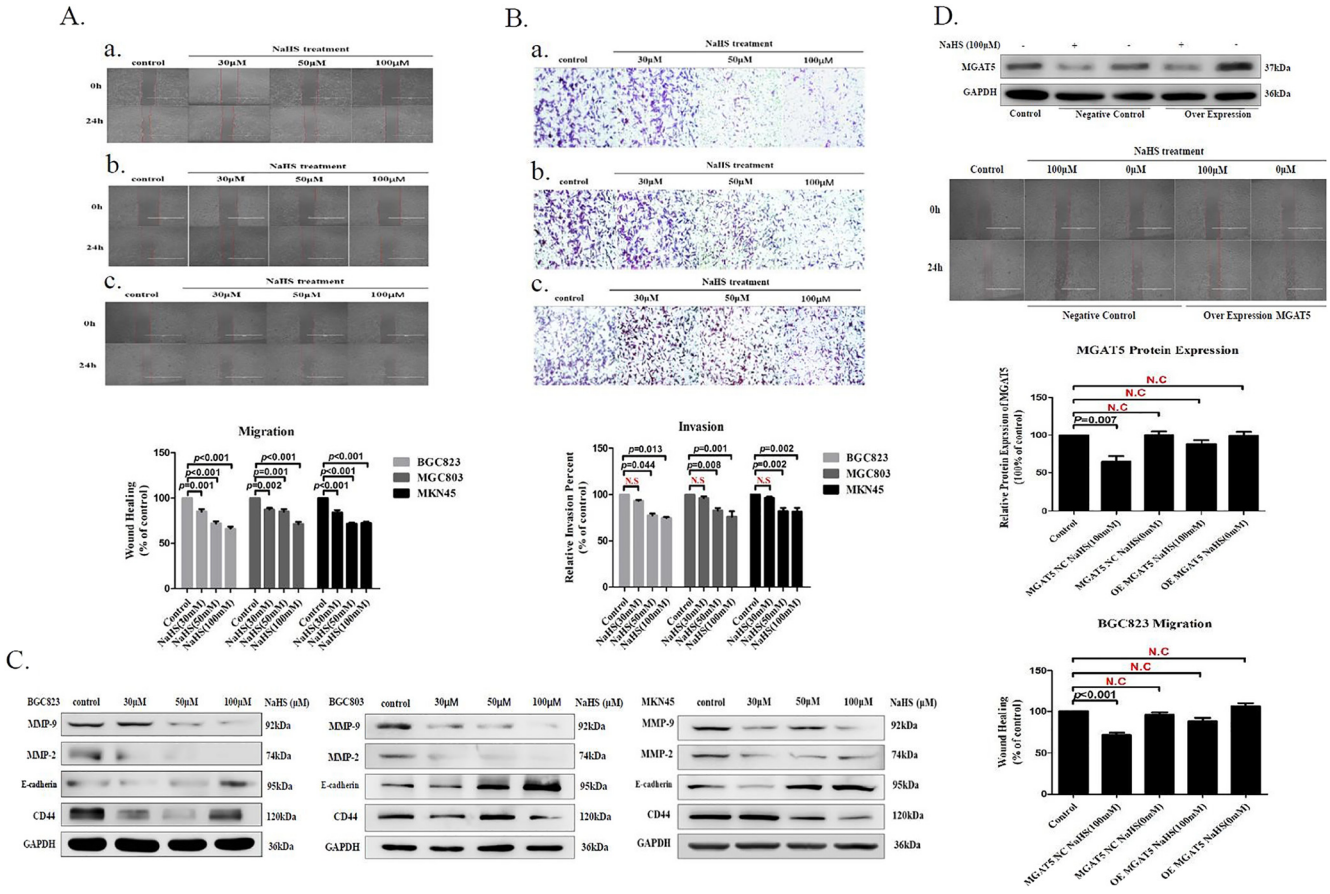

Figure 4. H_2S inhibits MGAT5-promoted GC cells migration and invasion.(A). Wound healing assayed that the inhibitory effect of H_2S to migration for serum free stimulated GC cells. Up panel: treatment of H_2S, the migration capacity was detected. *a*. BGC823, *b*. MGC803, and *c*. MKN45. Down panel: quantification of the inhibition activity of H_2S on migration. (B). Transwell assayed that the inhibitory effect of H_2S to invasion for serum free stimulated GC cells. Up panel: treatment of H_2S, the invasion capacity was detected. *a*. BGC823, *b*. MGC803, and *c*. MKN45. Down panel: quantification of the inhibition activity of H_2S on invasion. (C). Western blotting assayed EMT relevant protein on GC cells after 24 hours of treatment with NaHS at various concentrations. GAPDH was used as a loading control. (D). The inhibitory effect of H_2S on migration of serum free stimulated MGAT5 over-expression in BGC823. Each bar represents the means ± S.D. of three independent experiments.

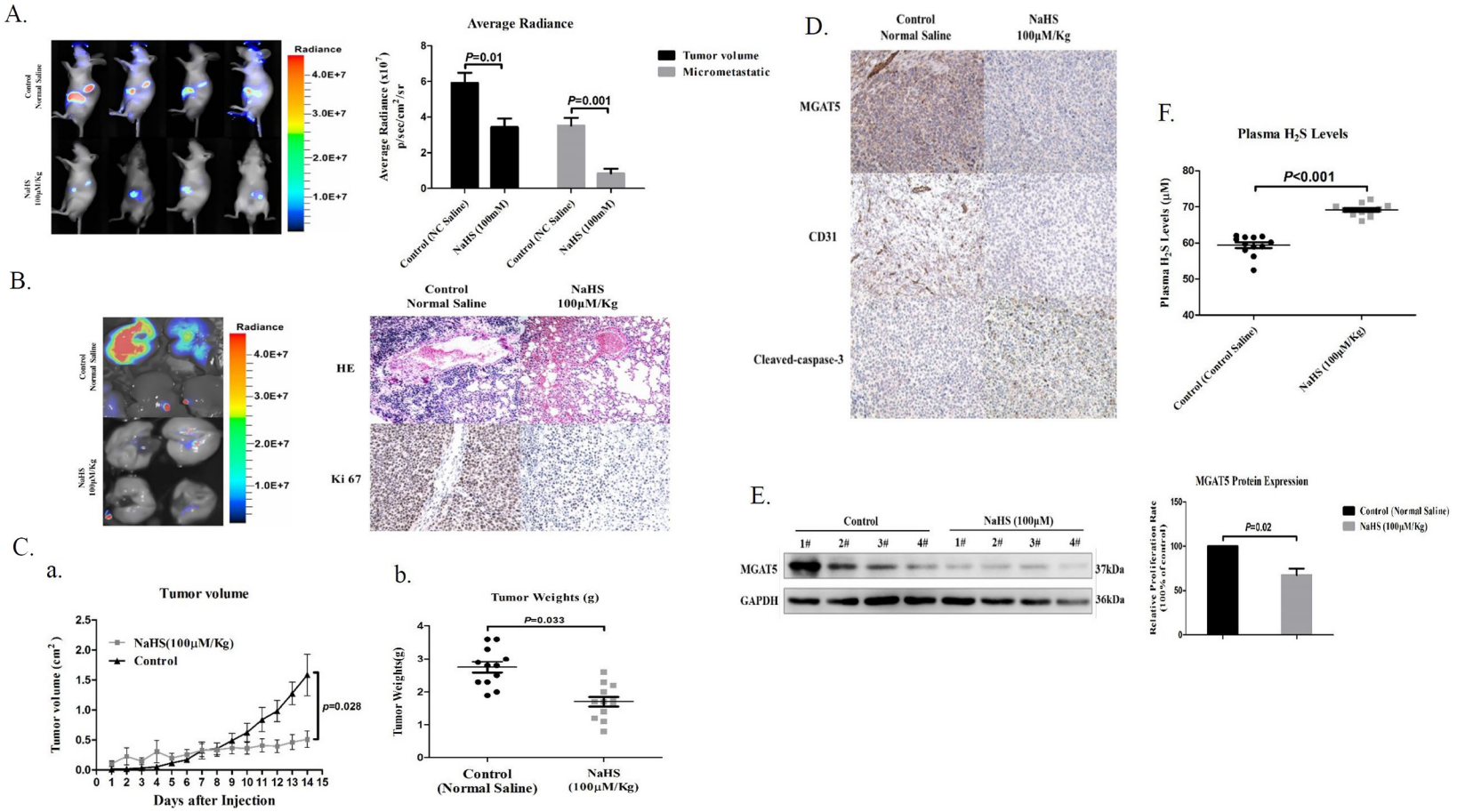

Figure 5. H_2S inhibits tumor growth and metastasis in gastric carcinoma Xenografts.(A). Effect of H_2S on lung metastasis of human gastric carcinoma cell BGC823 in mice orthotopic Xenotransplantation model. Left. representative bioluminescence imaging of metastatic nodules on lungs. Right. The BGC823 colonies were measured. (n = 3 flanks and 4 mice in each group). (B). Effect of H_2S on lung metastasis of human gastric carcinoma cell BGC823 in mice orthotopic Xenotransplantation model. Left. representative bioluminescence imaging of metastatic nodules on lungs. Right. HE staining and IHC staining of Ki67 representative photograph of metastatic nodules on lungs. (C). Tumor growth inhibition upon H_2S treatment in BGC823 gastric carcinoma mice subcutaneous Xenografts tumor model. *a*. The curve of tumor growth after 15-days treatment of H_2S. *b.* Experimental inhibitory effects of H_2S on BGC823 Xenografts in nude mice. The percentage of relative tumor volume inhibition values was measured on the last day during the experiment. (D). Effect of H_2S against primary tumor growth and angiogenesis. A typical photograph of IHC staining of MGAT5, CD31, and cleaved-caspase-3. (E). Inhibition of the expression of MGAT5 in BGC823 mice orthotopic Xenotransplantation model by H_2S. Mice were humanely euthanized on the last day at 2 hours post-administration of H_2S and the tumors were resected. Equal amounts of proteins of tumor tissues were evaluated for expression of MGAT5 levels. (F). The level of H_2S in the plasma of mice orthotopic Xenotransplantation model. Data are shown as means ± S.D. (n = 3 flanks and 4 mice in each group).

the level of ROS by chemiluminescence analysis with the same amount of GC cells protein at the same time with NaHS treatment on different concentrations. We found the H_2S promoted a decreased cellular level of the ROS in GC cells (Figure 3H). To test whether the H_2S suppressed GC cells growth by targeting inhibited the activity of MGAT5, we verification of the impact on glycolysis function, ATP production, and fatty acid oxidation of GC cells stably expressing MGAT5. We found that MGAT5 overexpression decreased the inhibitory effect on GC cells glycolysis function, ATP production, and fatty acid oxidation with H_2S treatment (Figure 3D, E, F, Supplementary Figure S3A). These results support our previous observation, indicating that of H_2S suppresses MGAT5-promoted GC cells growth *in vitro.*

H_2S Inhibits MGAT5-Promoted GC Cells Migration and Invasion

Metastasis is a major conundrum in Oncotherapy. Cancer cells must invade surrounding tissues and extravasate through the endothelium to blood or lymphatic circulation during the metastasis [10–12]. We found that H_2S significantly inhibited MGAT5-promoted GC cells migration and invasion on different concentrations (Figure 4A, B). Epithelial mesenchymal transition (EMT) is the initial and key step for cancer metastasis. During EMT, cancer cell phenotype changes with a series of proteins, including epithelial and mesenchymal markers [38,39]. Western blot detection indicated that H_2S significantly downregulated the expression of CD44 while upregulated the expression of E-cadherin from GC cells (Figure 4C). Meanwhile, MMP-9 and MMP-2 also remarkably downregulated by NaHS treatment from GC cells (Figure 4C). To testify whether the H_2S inhibited migration by targeting impaired the activity of MGAT5, we examined the impact on migration of BGC823 cells stably expressing MGAT5. We found that MGAT5 overexpression decreased the inhibitory effect on BGC823 cells migration with H_2S treatment (Figure 4D). These results manifested that H_2S showed migration and invasion inhibitory effects in MGAT5-promoted GC cells.

H_2S Inhibits Tumor Growth and Metastasis in Gastric Carcinoma Xenografts

To determine whether H_2S inhibits GC growth and metastasis *in vivo*, we established mice subcutaneous Xenograft tumor model and mice orthotopic Xenotransplantation model with BGC823 cells. When tumors were palpable, mice were randomized to receive either control (Normal Saline) or NaHS by every other daily injection. H_2S

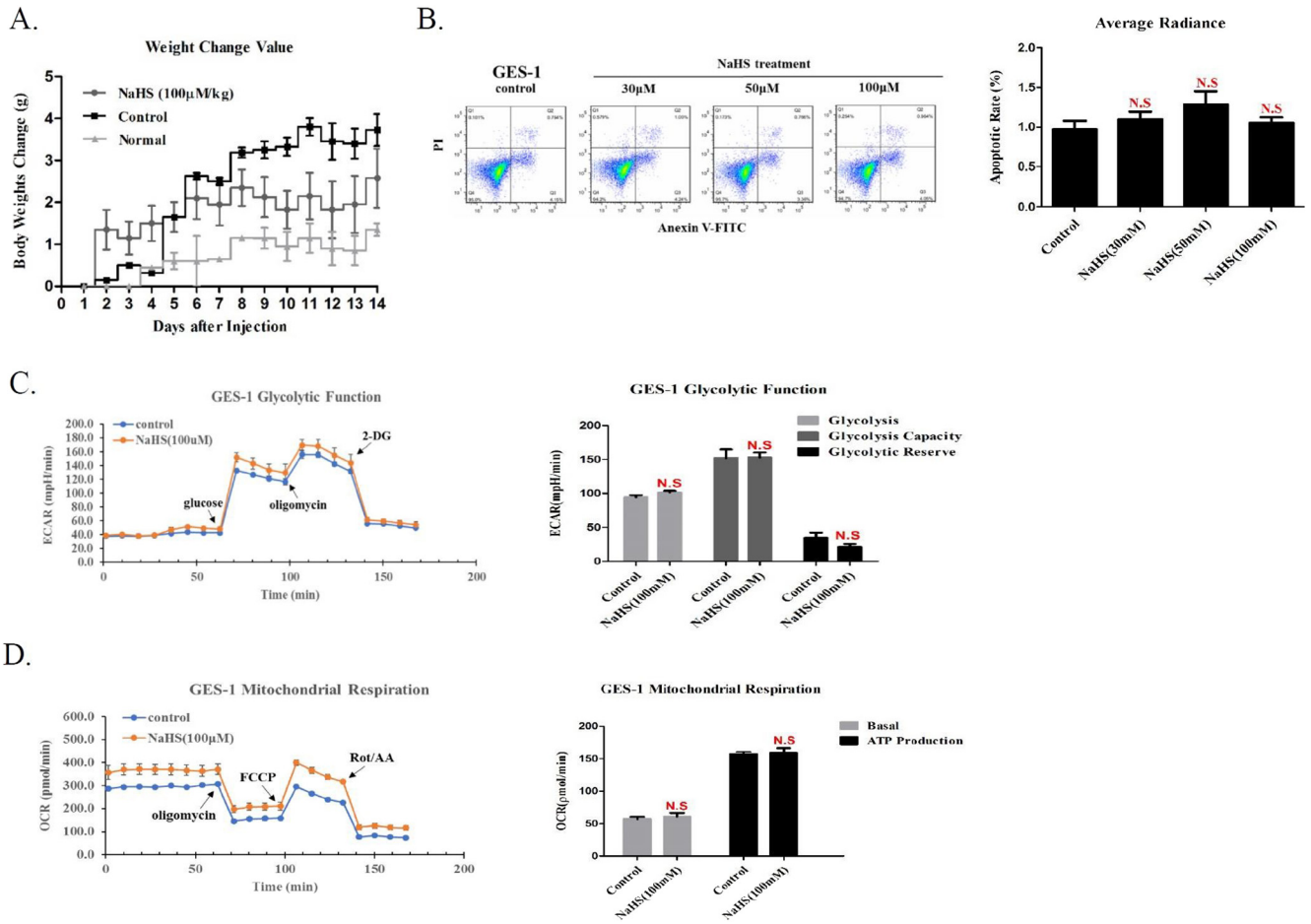

Figure 6. The potential toxicity of H_2S *in vitro* and *in vivo*.(A). Body weight of tumor-bearing mice measured at the indicated times. Apoptotic and metabolism assayed at the indicated concentration by FACS and Seahorse XF24 extracellular Flux Analyzer in human normal gastric cells GES-1. (B). Representative FACS plots and quantitative data of apoptotic rate. Treatment of H_2S, (C). Glycolysis Function and (D). Mitochondrial Respiration rates were detected. Each bar represents the means ± S.D. of three independent experiments.

administered at 100 μM/Kg significantly inhibited gastric carcinoma growth both in mice subcutaneous Xenograft tumor model and mice orthotopic Xenotransplantation model, as tumor weight was markedly reduced in NaHS treatment groups compared with control groups in mice subcutaneous Xenograft tumor model (Figure 5A, C). Notably, the lung metastasis was significantly reduced in mice that received NaHS (Figure 5A, B). In order to carry out mechanism research, tumor tissues were either prepared for western blot or immunohistochemistry (IHC) analysis. We found H_2S inhibited MGAT5 expression in high- and low- dose groups by western blot assay (Figure 5E). IHC analysis also showed that H_2S significantly reduced MGAT5 level *in vivo* (Figure 5D). Moreover, we also found the reduction of tumor vascular density and increase the expression of cleaved-caspase-3 in NaHS treatment group (Figure 5D). Finally, we detected the level of H_2S in the plasma of mice. Compared with the control group (average 58.526 μM), the treatment group was significantly higher than the control group (average 69.618 μM) (Figure 5F). Taken together, these data demonstrated that H_2S is detrimental to the growth and metastasis of gastric carcinoma in the preclinical mice subcutaneous Xenograft tumor model and mice orthotopic Xenotransplantation model.

The Potential Toxicity of H_2S In Vitro and In Vivo

In vivo, we had injected the tumor-bearing mice with a dose of NaHS 100 μM/Kg for 15 days which did not cause their weight loss and death, indicating the safety of H_2S suppressing the growth and metastasis of BGC823 cells in mice subcutaneous Xenograft tumor model and mice orthotopic Xenotransplantation model (Figure 6A). *In vitro,* we measured cell apoptosis and metabolism for human normal gastric epithelial cells GES-1 with NaHS treatment. We found that H_2S has no obvious adverse effects at our therapeutic concentration (Figure 6B, C, D, Supplementary Figure S6A). In contrast with a high concentration of H_2S, these data demonstrated that low concentration of H_2S may have no obvious adverse effects *in vitro* and *in vivo.*

Discussion

H_2S plays an important role in many physiological and pathophysiological processes in mammals [16,17]. However, the effect of H_2S on cancer about its development and progression remains largely unclear. We proposed that relatively low concentration of exogenous H_2S could inhibit GC cells growth and metastasis, which may help us increasingly recognize pharmacological activities of H_2S, including inhibit growth and metastasis in GC cells. In this study, we identified MGAT5 as one of the potential target of H_2S and demonstrated H_2S associated anti-tumor activities, particularly inhibit growth and metastasis, which may help understand the broad anti-tumor function of H_2S.

Unlike normal cells, MGAT5 overexpress cancer cells were more sensitive to inhibition MGAT5 expression [11,21,33,38]. As an appealing target for cancer therapy, the efforts for the discovery of MGAT5 inhibitor has not been very successful, the problem is mainly focused on its effectiveness, adverse reactions, and Drug Resistance. It would be interesting to further seek whether this strategy could lead to MGAT5 inhibitor with improved anti-tumor properties.

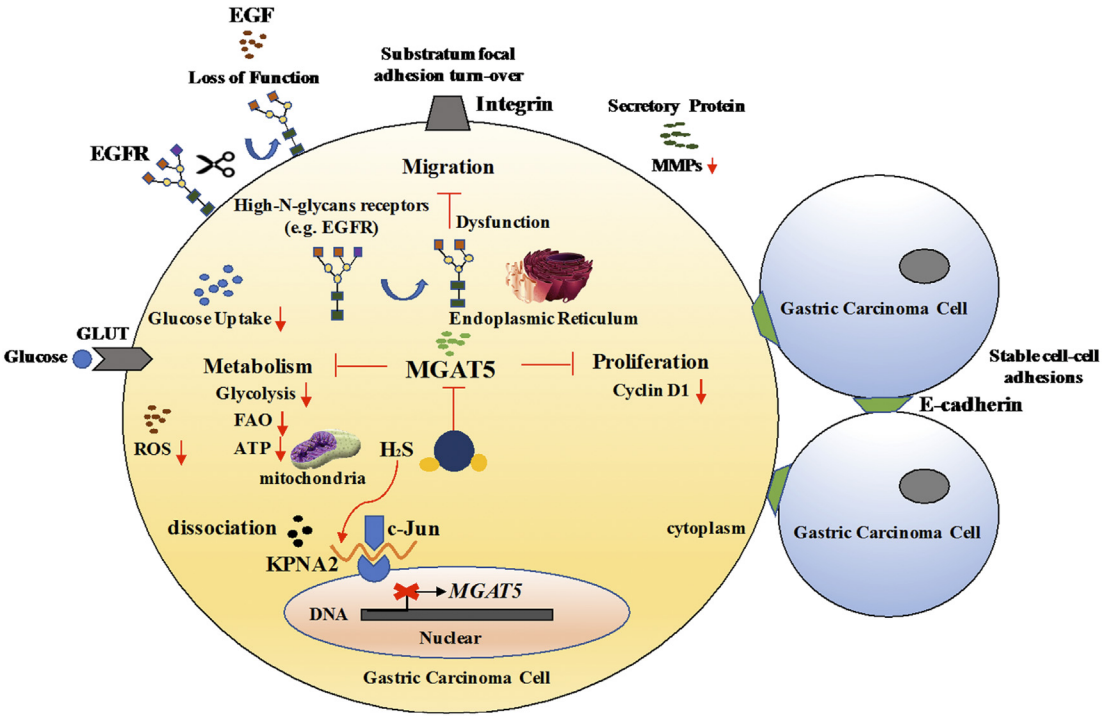

Figure 7. Hydrogen Sulfide demonstrates promising antitumor efficacy in gastric carcinoma by targeting MGAT5.Schematic illustration of our systems biology approach to identify H_2S may be an important MGAT5 inhibitor and their corresponding targets. H_2S specifically dissociation of KPNA2 with c-Jun interaction, and blocking c-Jun nuclear translocation, and downregulation of MGAT5 expression at the level of gene and protein. H_2S inhibited MGAT5 activity lead to suppress metabolism, substratum focal adhesion turn-over, reduce the expression of exclusively abnormal glycoprotein processes, and disturb cell cyclin. It provides insights into a better understanding of the molecular mechanisms of H_2S in anti-cancer effects which are required for further application in translational medicine.

In summary, our results show that H_2S may be an important MGAT5 suppressor, inhibits MGAT5-promoted tumor growth and metastasis, both *in vitro* and *in vivo*. Furthermore, there were no obvious adverse effects *in vitro* and *in vivo* at our therapeutic concentration. This study provides new insights for a better understanding of the mechanisms of H_2S in anti-tumor growth and metastasis effects (Figure 7). Most safely novel slow-releasing H_2S donors and H_2S-releasing hybrid drugs will be designed and applied for further anti-tumor research.

Supplementary data to this article can be found online at https://doi.org/10.1016/j.tranon.2018.04.008.

Acknowledgments

We acknowledge the elder sister of our favorites, Rui Wang wants to thank, in particular, the patience, care and support from Beibei Tao over the past three years. In addition, on the occasion of the 10th anniversary marriage, this article is dedicated to my beloved wife, and bless us to be happiness and satisfaction forever.

References

[1] Freddie B, Ahmedin J, Nathan G, Jacques F, and David F (2012). Global cancer transitions according to the Human Development Index (2008-2030): a population-based study. *Lancet Oncol* **13**, 790–801.

[2] Huang B, Sun Z, Wang Z, Lu C, Zhao B, and Xu H (2013). Factors associated with peritoneal metastasis in non-serosa-invasive gastric cancer: a retrospective study of a prospectively-collected database. *BMC Cancer* **131**, 57.

[3] Croci DO, Cerliani JP, Dalottomoreno T, Mendezhuergo SP, Mascanfroni ID, Dergandylon S, and Rabinovich GA (2014). Glycosylation-Dependent Lectin-Receptor Interactions Preserve Angiogenesis in Anti-VEGF Refractory Tumors. *Cell* **156**, 744–758.

[4] Granovsky M, Fata JE, Pawling J, Muller WJ, Khokha R, and Dennis JW (2000). Suppression of tumor growth and metastasis in Mgat5-deficient mice. *Nat Med* **6**, 306–312.

[5] Partridge EA, Roy CL, Guglielmo GM, Pawling J, Cheung P, Granovsky M, and Dennis JW (2004). Regulation of cytokine receptors by Golgi N-glycan processing and endocytosis. *Science* **306**, 120–124.

[6] Lau KS and Dennis JW (2008). N-Glycans in cancer progression. *Glycobiology* **18**, 750–760.

[7] Dennis JW, Pawling J, Cheung P, Partridge E, and Demetriou M (2002). UDP-N-acetylglucosamine: α-6-d-mannoside β1,6 N-acetylglucosaminyltransferase V (Mgat5) deficient mice. *Biochim Biophys Acta* **1573**, 414–422.

[8] Demetriou M, Granovsky M, Quaggin S, and Dennis JW (2001). Negative regulation of T-cell activation and autoimmunity by Mgat5 N-glycosylation. *Nature* **409**, 733–739.

[9] Morgan RW, Gao G, Pawling J, Dennis JW, Demetriou M, and Li B (2004). N-Acetylglucosaminyltransferase V (Mgat5)-Mediated N-Glycosylation Negatively Regulates Th1 Cytokine Production by T Cells. *J Immunol* **173**, 7200–7208.

[10] Kang Y and Massague J (2004). Epithelial-mesenchymal transitions: twist in development and metastasis. *Cell* **118**, 277–279.

[11] Mendelsohn R, Cheung P, Berger L, Partridge EA, Lau KS, Datti A, and Dennis JW (2007). Complex N-Glycan and Metabolic Control in Tumor Cells. *Cancer Res* **67**, 9771–9780.

[12] Junior JC and Morgadodiaz JA (2016). The role of N-glycans in colorectal cancer progression: potential biomarkers and therapeutic applications. *Oncotarget* **7**, 19395–19413.

[13] Szabo C (2007). Hydrogen sulphide and its therapeutic potential. *Nat Rev Drug Discov* **611**, 917–935.

[14] Wallace JL and Wang R (2015). Hydrogen sulfide-based therapeutics: exploiting a unique but ubiquitous gasotransmitter. *Nat Rev Drug Discov* **145**, 329–345.

[15] Yang G, Wu L, Jiang B, Yang W, Qi J, Cao K, and Wang R (2008). H_2S as a Physiologic Vasorelaxant: Hypertension in Mice with Deletion of Cystathionine γ-Lyase. *Science* **322**, 587–590.

[16] Barr LA and Calvert JW (2014). Discoveries of Hydrogen Sulfide as a Novel Cardiovascular Therapeutic. *Circulation* **789**, 2111–2118.

[17] Tao BB, Liu SY, Zhang CC, Fu W, Cai WJ, Wang Y, Shen Q, Wang MJ, Chen Y, and Zhang LJ, et al (2013). VEGFR2 functions as an H_2S-targeting Receptor Protein kinase with its novel Cys1045-Cys1024 disulfide bond serving as a specific molecular switch for hydrogen sulfide actions in Vascular endothelial cells. *Antioxid Redox Signal* **19**, 448–464.

[18] Zhang L, Qi Q, Yang J, Sun D, Li C, Xue Y, Jiang QY, Tian Y, Xu CQ, and Wang R (2015). An Anticancer Role of Hydrogen Sulfide in Human Gastric Cancer Cells. *Oxidative Med Cell Longev* , 636410.

[19] Atteneramos MS, Wagner ED, Gaskins HR, and Plewa MJ (2007). Hydrogen Sulfide Induces Direct Radical-Associated DNA Damage. *Mol Cancer Res* **5**, 455–459.

[20] Lee Z, Teo X, Tay EY, Tan C, Hagen T, Moore PK, and Deng L (2014). Utilizing hydrogen sulfide as a novel anti-cancer agent by targeting cancer glycolysis and pH imbalance. *Br J Pharmacol* **171**, 4322–4336.

[21] Lange T, Ullrich S, Müller I, Nentwich MF, Stübke K, Feldhaus S, Knies C, Hellwinkel QL, Vessella RL, and Abramjuk C, et al (2012). Human Prostate Cancer in a Clinically Relevant Xenograft Mouse Model: Identification of β (1,6)-Branched Oligosaccharides as a Marker of Tumor Progression. *Clin Cancer Res* **18**, 1364–1373.

[22] Taniguchi N and Kizuka Y (2015). Chapter Two–Glycans and Cancer: Role of N-Glycans in Cancer Biomarker, Progression and Metastasis, and Therapeutics. *Adv Cancer Res* **126**, 11.

[23] Zhao Y, Takahashi M, Gu J, Miyoshi E, Matsumoto A, Kitazume S, and Taniguchi N (2008). Functional roles of N-glycans in cell signaling and cell adhesion in cancer. *Cancer Sci* **99**, 1304–1310.

[24] Saito H, Gu J, Nishikawa A, Ihara Y, Fujii J, Kohgo Y, and Taniguchi N (1995). Organization of the human N-acetylglucosaminyltransferase V gene. *J Biochem* **233**, 18–26.

[25] Schumacker PT (2011). SIRT3 Controls Cancer Metabolic Reprogramming by Regulating ROS and HIF. *Cancer Cell* **19**, 299–300.

[26] Zhou L, Tan A, Iasvovskaia S, Li J, Lin A, and Hershenson MB (2003). Ras and Mitogen-Activated Protein Kinase Kinase Kinase-1 Coregulate Activator Protein-1 and Nuclear Factor-κB Mediated Gene Expression in Airway Epithelial Cells. *Am J Respir Cell Mol Biol* **28**, 762–769.

[27] Chook YM and Blobel G (2011). Karyopherins and nuclear import. *Curr Opin Struct Biol* **116**, 703–715.

[28] Pemberton LF and Paschal BM (2005). Mechanisms of Receptor-Mediated Nuclear Import and Nuclear Export. *Traffic* **63**, 187–198.

[29] Karin M (1995). The Regulation of AP-1 Activity by Mitogen-activated Protein Kinases. *J Biol Chem* **270**, 16483–16486.

[30] Laplante M and Sabatini DM (2012). mTOR signaling in growth control and disease. *Cell* **149**, 274–293.

[31] Warburg O (1956). On the Origin of Cancer Cells. *Science* **123**, 309–314.

[32] Hsu PP and Sabatini DM (2008). Cancer Cell Metabolism: Warburg and Beyond. *Cell* **134**, 703–707.

[33] Vander Heiden MG, Cantley LC, and Thompson CB (2009). Understanding the Warburg effect: the metabolic requirements of cell proliferation. *Science* **324**, 1029–1033.

[34] Christofk HR, Vander Heiden MG, Harris MH, Ramanathan A, Gerszten RE, and Wei R (2008). The M2 splice isoform of pyruvate kinase is important for cancer metabolism and tumour growth. *Nature* **452**, 230–233.

[35] Soga T (2013). Cancer metabolism: Key players in metabolic reprogramming. *Cancer Sci* **104**, 275–281.

[36] Yang Y, Karakhanova S, Hartwig W, Dhaese JG, Philippov PP, Werner J, and Bazhin AV (2016). Mitochondria and Mitochondrial ROS in Cancer: Novel Targets for Anticancer Therapy. *J Cell Physiol* **231**, 2570–2581.

[37] Johswich A, Longuet C, Pawling J, Rahman AM, Ryczko M, Drucker DJ, and Dennis JW (2014). N-Glycan Remodeling on Glucagon Receptor Is an Effector of Nutrient Sensing by the Hexosamine Biosynthesis Pathway. *J Biol Chem* **289**, 15927–15941.

[38] Deng Q, Chen Y, Yin N, Shan N, Luo X, Tong C, Zhang H, Philip NB, Liu X, and Qi H (2015). N-acetylglucosaminyltransferase V inhibits the invasion of trophoblast cells by attenuating MMP2/9 activity in early human pregnancy. *Placenta* **36**, 1291–1299.

[39] Yang HM, Yu C, and Yang Z (2012). N-acetylglucosaminyltransferase v negatively regulates integrin α5β1-mediated monocyte adhesion and transmigration through Vascular Endothelium. *Int J Oncol* **41**, 589–598.